Detection of a geostationary satellite with the Navy Prototype Optical Interferometer

J.T. Armstrong[*a], R.B. Hindsley[a], H.R. Schmitt[b], F.J. Vrba[c], J.A. Benson[c], D.J. Hutter[c], R.T. Zavala[c]

[a]Naval Research Laboratory, Code 7215, 4555 Overlook Ave., SW,
Washington, DC, USA 02375;
[b]Computational Physics, Inc., 8001 Braddock Rd., Suite 210,
Springfield, VA, USA 2251;
[c]US Naval Observatory, Flagstaff Station, 10391 W. Observatory Rd.,
Flagstaff, AZ, USA 86001 USA

ABSTRACT

We have detected a satellite via optical interferometry for the first time, using a 16 m baseline of the Navy Prototype Optical Interferometer (NPOI) to observe the geostationary communications satellite DirecTV-9S during the "glint" seasons of February–March 2008 and 2009 when the sun-satellite-NPOI geometry was favorable for causing specular reflections from geostationary satellites. We used the US Naval Observatory Flagstaff Station 1 m telescope to generate accurate positions for steering the NPOI. Stars are the easiest targets for optical/infrared interferometers because of their high surface brightness. Low surface brightness targets are more difficult: if they are small enough not to be resolved out by typical baselines, they are likely to be too faint to produce detectable fringes in an atmospheric coherence time. The 16 m NPOI baseline, the shortest available at the time of our observations, resolves out structures larger than ~ 1.5 m at the geostationary distance, while a typical size for the solar panel arrays is 2 m $\times$ 30 m. Our detection indicates that a small fraction of the satellite glinted, not surprising given that the solar panels are not accurately flat. Our fringe data are consistent with a two-component image consisting of a 1 to 1.3 m higher surface brightness component and a significantly larger lower surface brightness component. The brightness of the glints ($2^{\rm m}4$ and $\lesssim 1^{\rm m}5$ for the two detections in March 2009) and the size scale suggest that the compact component has an albedo of 0.06 to 0.13, while the larger-scale component is much darker, if circular geometry is assumed.

Keywords: optical interferometry, NPOI, geostationary satellites

1. THE NPOI

The Navy Prototype Optical Interferometer (NPOI),[1] a collaborative project of the Naval Research Laboratory and the US Naval Observatory in partnership with Lowell Observatory, is a multi-element long-baseline optical interferometer located at the Lowell Observatory dark-sky site on Anderson Mesa, near Flagstaff, Arizona (see Fig. 1). The NPOI was designed for both wide-angle astrometry with milliarcsecond precision and milliarcsecond imaging of stars, stellar surfaces, and circumstellar material. First fringes were obtained in 1994, and the first six-way interferometric observations were done in 2001. An aerial view of the NPOI is shown in Fig. 1.

The NPOI is a group-delay tracking interferometer, which increases its on-fringe efficiency but requires tracking the fringes rather than scanning through the delay range where the fringes are expected to be. For imaging observations, up to six array elements (siderostats) can be used, although it is common to use three to five elements. The imaging array consists of two moveable elements, with a third expected in the summer of 2010 and three more under development. The astrometric array elements can also be used in imaging observations. The astrometric array consists of four fixed array elements equipped with laser metrology to monitor the motions of the siderostats as they track.

---

[*]tom.armstrong@nrl.navy.mil; phone 1 202 767 0669; fax 1 202 404 8894

Report Documentation Page

Public reporting burden for the collection of information is estimated to average 1 hour per response, including the time for reviewing instructions, searching existing data sources, gathering and maintaining the data needed, and completing and reviewing the collection of information. Send comments regarding this burden estimate or any other aspect of this collection of information, including suggestions for reducing this burden, to Washington Headquarters Services, Directorate for Information Operations and Reports, 1215 Jefferson Davis Highway, Suite 1204, Arlington VA 22202-4302. Respondents should be aware that notwithstanding any other provision of law, no person shall be subject to a penalty for failing to comply with a collection of information if it does not display a currently valid OMB control number.

1. REPORT DATE **JUL 2010**	2. REPORT TYPE	3. DATES COVERED **00-00-2010 to 00-00-2010**

4. TITLE AND SUBTITLE **Detection Of A Geostationary Satellite With The Navy Prototype Optical Interferometer**	5a. CONTRACT NUMBER
	5b. GRANT NUMBER
	5c. PROGRAM ELEMENT NUMBER
6. AUTHOR(S)	5d. PROJECT NUMBER
	5e. TASK NUMBER
	5f. WORK UNIT NUMBER
7. PERFORMING ORGANIZATION NAME(S) AND ADDRESS(ES) **Naval Research Laboratory,Code 7215,4555 Overlook Ave.SW,Washington,DC,02375**	8. PERFORMING ORGANIZATION REPORT NUMBER
9. SPONSORING/MONITORING AGENCY NAME(S) AND ADDRESS(ES)	10. SPONSOR/MONITOR'S ACRONYM(S)
	11. SPONSOR/MONITOR'S REPORT NUMBER(S)

12. DISTRIBUTION/AVAILABILITY STATEMENT
Approved for public release; distribution unlimited

13. SUPPLEMENTARY NOTES

14. ABSTRACT
We have detected a satellite via optical interferometry for the first time, using a 16 m baseline of the Navy Prototype Optical Interferometer (NPOI) to observe the geostationary communications satellite DirecTV-9S during the ?glint? seasons of February?March 2008 and 2009 when the sun-satellite-NPOI geometry was favorable for causing specular reflections from geostationary satellites. We used the US Naval Observatory Flagstaff Station 1 m telescope to generate accurate positions for steering the NPOI. Stars are the easiest targets for optical/infrared interferometers because of their high surface brightness. Low surface brightness targets are more difficult: if they are small enough not to be resolved out by typical baselines, they are likely to be too faint to produce detectable fringes in an atmospheric coherence time. The 16 m NPOI baseline, the shortest available at the time of our observations, resolves out structures larger than ∼ 1.5 m at the geostationary distance, while a typical size for the solar panel arrays is 2 m ?30 m. Our detection indicates that a small fraction of the satellite glinted, not surprising given that the solar panels are not accurately flat. Our fringe data are consistent with a two-component image consisting of a 1 to 1.3 m higher surface brightness component and a significantly larger lower surface brightness component. The brightness of the glints (2.m 4 and 1.m 5 for the two detections in March 2009) and the size scale suggest that the compact component has an albedo of 0.06 to 0.13, while the larger-scale component is much darker, if circular geometry is assumed.

15. SUBJECT TERMS

16. SECURITY CLASSIFICATION OF:			17. LIMITATION OF ABSTRACT	18. NUMBER OF PAGES	19a. NAME OF RESPONSIBLE PERSON
a. REPORT **unclassified**	b. ABSTRACT **unclassified**	c. THIS PAGE **unclassified**	**Same as Report (SAR)**	**8**	

Figure 1. The Navy Prototype Optical Interferometer (NPOI). The north arm is the one extending to the left of the center of the array. Feed pipes lead from the array center to the optics laboratory, which houses the continuously-adjustable "fast delay lines." Extending to the north of the optics laboratory is the array of "long delay lines" that will provide additional delay when the longest baselines are commissioned. Close to the center of the array are the four enclosures for the astrometric array elements, which are fixed in position. The east and center astrometric array elements were used for these observations, along with one of the moveable imaging array elements, E6, visible just above and to the right of the east astrometric enclosure. Photo courtesy of Michael Collier.

2. GEOSATS AND GLINTS

Geostationary satellites (geosats) have become indispensible for communications, surveillance, and environmental and weather observations. Direct imaging of these satellites could be helpful in diagnosing problems when they arise, but at an altitude of nearly 35800 km, 1 m subtends 5 milliarcseconds (mas), so even the ~ 40 m span of the largest solar panels is considerably less than an arc second in size and is at or beyond the resolution limit of all but the largest adaptive-optics equipped telescopes.

A few of the many geosat configurations that have been placed in orbit are shown in Fig. 2. Geosats are faint—roughly 14th magnitude—almost all the time. However, some types can glint brightly for a few minutes a day during twice-yearly "glint seasons" lasting about a week. These types consist of a central bus and two extended solar-panel arrays. The solar arrays are oriented north-south, with the normal to the panels pointing to the the right ascension of the mean Sun. The alignment with the Sun is not exact: first, the Sun's true right ascension differs from that of the mean Sun by up to $\pm 4°$ depending on the time of year, and second, early in a satellite's life, when the panels are most efficient, they may be pointed several degrees away from the mean Sun in order to avoid generating excess power or solar heating.

Satellites of this type can glint brightly when the Sun reflects specularly from the solar panels; it's as if we see the Sun reflected in a mirror, although the panels are not optically flat. Therefore, these glints can occur only when the declination δ of the satellite as seen from a given location is close to the declination of the Sun. From Flagstaff, geostationary satellites are at $\delta = -5°6$, so the glint seasons are somewhat before the spring equinox and somewhat after the fall equinox, or approximately 26 February–4 March and 7–14 October.

During glint season, a satellite with panels pointed toward the Sun may glint when the azimuth of the Sun (which is below the horizon) is 180° from that of the satellite, when the Earth's shadow covers the satellite. Only at the beginning of the (northern hemisphere) spring season or the end of the fall season—when the Sun is slightly south of $\delta = -5°6$, so the Earth's shadow passes north of the satellite—can a glint take place. However, if the panels are pointed away from the Sun, the glint takes place before or after the Earth's shadow covers the
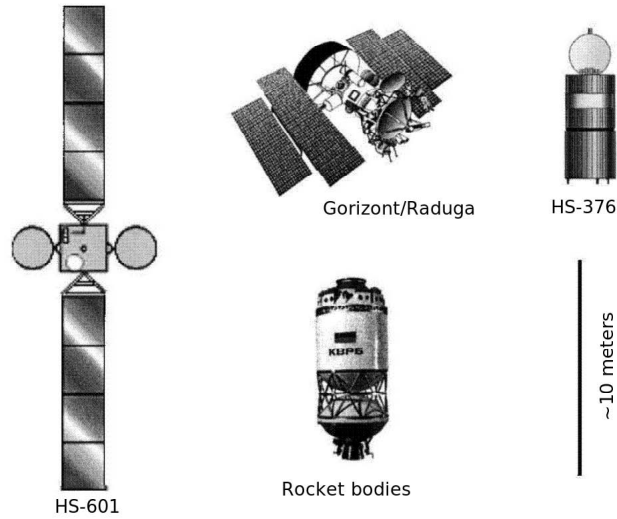
Figure 2. A few of the many types of satellite in geostationary orbit. The satellite detected in this study, DirecTV-9S, is similar to the HS-601 type shown here, in that it has two long, narrow solar-panel arrays. Typically, such satellites have the long dimension of panels oriented north-south, with the normal to the panels pointed at or close to the Sun. This figure is taken from Ref. 2.

satellite. This is the case for DirecTV-9S, the satellite that we detected with the NPOI in March 2008 and March 2009.

The glint light curves shown in Fig. 3 demonstrate these two behaviors. AMSC1 entered the Earth's shadow before the glint reached maximum brightness, while DirecTV-1R had already passed through the shadow when it peaked.
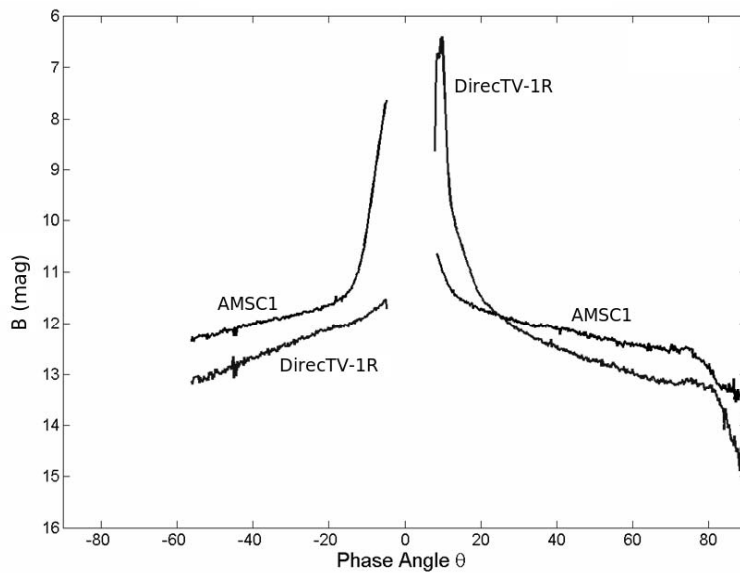

Figure 3. Light curves of two typical glinting satellites. The gap around $\theta = 0°$ is due to the satellites passing through the Earth's shadow. The normal to the solar panels does not point directly toward the Sun for either satellite; for DirecTV-1R, the tilt away from the Sun is large enough to move the peak of the glint out of Earth shadow.

The theoretical peak magnitude m_g(peak) of a glint can be calculated from the apparent magnitude of the

Sun, the area of the solar panels, and their albedo.[3] For a panel area of 100 m^2 and an albedo A of 0.1, m_g(peak) is about $-3^{\mathrm{m}}4$, much brighter than the observed peak magnitudes. The primary reason for this relative faintness is probably the lack of local or large-scale flatness of the solar panels.

3. INTERFEROMETRIC OBSERVATIONS

Observing geosats with an optical interferometer presents us with several challenges. The first is the glints themselves. Not all satellites glint, and predicting whether a given satellite will glint is not straightforward. If a satellite does glint, the glint may be extinguished by the Earth's shadow. And if the glint happens outside Earth's shadow, the time during which it is bright enough to observe is usually only a few minutes. A second challenge is the size of the satellite. Size scales of ~ 1.5 m or more will be resolved out on our 15.9 m baseline, producing very weak to no fringes.

The short duration presents a third challenge: finding the fringes before the glint fades. In order to keep the fringe search time shorter than the glint duration, we must set the delay lines within ~ 300 μm of the correct position, which in turn requires knowledge of the satellite position to better than one arcsecond for the 15.9 m baseline. The published orbital elements (the "two-line elements" [TLEs], available at http://celestrak.com) are not precise enough, and the satellite operators can, and sometimes do, move the satellite to a different longitude. In addition, the orbits are not perfectly geostationary; we found that drift rates of $0\rlap{.}{''}5$ min^{-1} in azimuth and elevation were not unusual.

To reduce the position uncertainties, and to monitor glints as they brightened, we did our own near-real-time astrometry,[4] using the US Naval Observatory Flagstaff Station (NOFS) 1 m Ritchey-Chretien telescope, about 19 km distant from the NPOI site. In each of the fields that we monitored, we used the TLEs and the program The Sky (http://www.bisque.com) to identify the satellites when there was more than one visible in the 20$'$ field of view. We continued observations until the glint became too bright for the detector, typically 20 min before maximum.

At the NPOI, we used the three array elements at stations E6, AE, and AC. Because of the beam combiner configuration, we could use only the E6–AE (15.9 m length at 93° azimuth) and AE–AC (18.9 m at $-68°$) baselines, so no closure phases were available. The complexity of coordinating the observations at the NOFS 1 m telescope and the NPOI led us to concentrate on a small number of targets, typically three to five each night.

Our first observing season, in 2007 October, produced experience and adjustments to the techniques, but no fringes. During our second season, in February–March 2008, we detected weak fringes on one target, DirecTV-9S, described in Ref. 5. The 2008 October session produced no detections, even though DirecTV-9S was one of the targets. However, in our fourth season, February–March 2009, we once more detected fringes in observations of DirecTV-9S. The signal-to-noise ratio in these 2009 fringes was considerably better than 2008. The fringe power spectrum, shown in Fig. 4, confirms the detection. In both 2008 and 2009, we detected fringes on only the 15.9 m baseline. We suspect that our non-detection on the 18.9 m baseline stems from the $\sim 25\%$ reduction in the squared fringe visibility, V^2, that results from the its greater length.

Our detection data consist of fringe amplitudes in 15 wavelength channels on only one baseline, too sparse to make an image. However, the trend of V^2 with wavelength can give us the approximate size scale of the glinting area, although having data on only an east-west baseline means that we have size information only along that direction. Fortunately for us, geosats of this general type are oriented with the long dimension of the solar panels north-south; if it were east-west, the satellite would be resolved out on this baseline.

The 2008 data indicated a size scale for the glinting area of roughly 1.3 m, but only the six reddest (lowest spatial resolution) channels had V^2 significantly different from 0. The 2009 visibilities are significantly non-zero in the reddest 11 channels and have much better signal-to-noise ratio. They are nearly constant across that span, suggesting an unresolved component, but the amplitudes are small ($V^2 \sim 0.07$), implying that a resolved component with a significant fraction of the total flux is diluting the fringes from the unresolved component.

We present the 2009 data in Fig. 5 as $|V|$ rather than the more conventional V^2 in order to show the contributions of the two components to the visibility. (The 2008 data are also consistent with these models, but the lower SNR of those data constrains the models poorly.) Since we do not have phase information, the
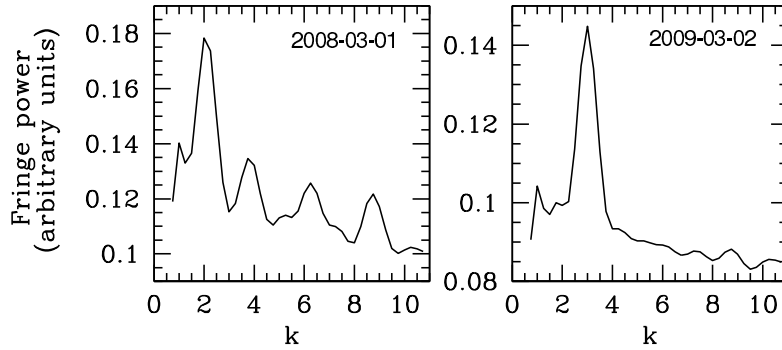
Figure 4. Fringe power spectra on the 15.9 m baseline. The abscissa, k, is the number of fringes per delay sweep stroke length measured in wavelengths. For the 2008 observations, the NPOI stroke on this baseline was two waves, while it was three waves in the 2009 observations. The power peaks at $k = 2$ and $k = 3$ in the respective data demonstrate that fringes were detected.

relative positions of these components is unknown; for example, they could be a patch of the solar panels plus an area of the bus. For purposes of the calculation, we assumed that the areas are circular, although we have no information in the north-south direction.
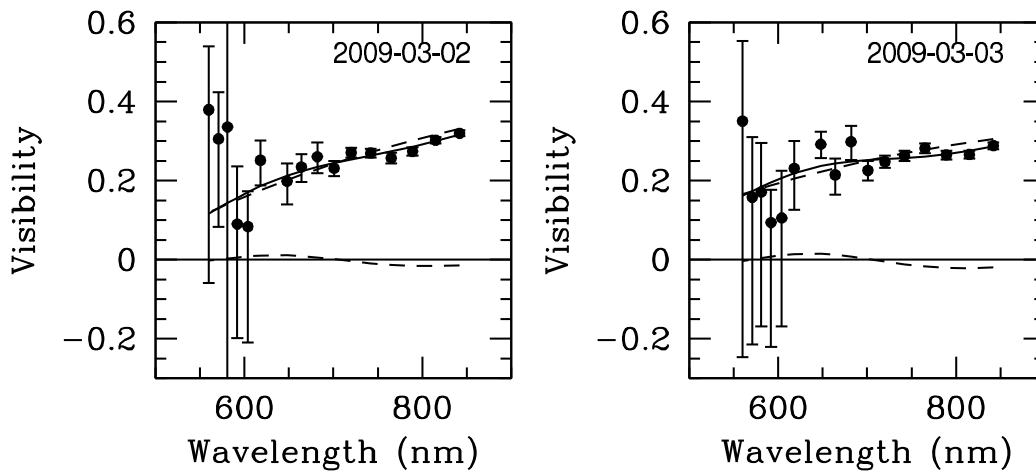

Figure 5. Observed visibility amplitudes in 2009, and two-component model visibilities. The visibilities $|V|$ (rather than the usual V^2) for the two detections in March 2009 are very similar, and can be fit with similar models consisting of one component of ~ 1 to 1.3 m (upper dashed curve in each panel) and a second component larger than ~ 3 m (lower dashed curves). The full curve shows the total visibility of the model.

Table 1 shows the parameters of the model fits to these data, as well as the peak glint magnitudes in the Cousins R band as observed at the NOFS 1 m telescope. (The detectors at the 1 m and at NPOI saturated at the peak brightness on 3 March.) The data do not constrain the size (L_2) of the larger component well, so we fit the size of the smaller component, L_1, and the fractional flux F_1 for three values of L_2. The fits from the two nights are quite similar, although the best fits for 3 March have a slightly smaller compact component that contributes a slightly smaller fraction of the total flux. For both nights, we obtained slightly better fits for $L_2 = 3.7$ m and 7 m than for the intermediate value of 5 m.

4. DISCUSSION

Are these size scales consistent with the glint magnitudes we observed? The maximum expected brightness of a glint can be estimated from the area and the albedo, as in the approach taken in Ref. 3 (see above). That

Table 1. Two-component model fits to March 2009 data

L_1 (m)	L_2 (m)	F_1/F_2	χ^2_ν	m_R(peak) (mag)
2 March 2009:				2.4
1.3	7	0.6 / 0.4	1.3	
1.2	5	0.45 / 0.55	1.8	
1.4	3.7	0.7 / 0.3	1.4	
3 March 2009:				< 1.5?
1.1	7	0.45 / 0.55	0.8	
0.6	5	0.25 / 0.75	1.0	
1.2	3.7	0.55 / 0.45	0.8	

approach can be inverted to estimate the albedo A, given the size scale L of the glinting area and the glint magnitude, m:

$$A = \left(\frac{\theta_0 H}{L} \right)^2 10^{0.4(m_0 - m)}, \tag{1}$$

where m_0 is the Sun's apparent magnitude ($-27^{\rm m}2$ in the R filter), θ_0 is the angular diameter of the Sun (0.009 rad), H is the distance to the satellite (about 35800 km for a geosat), and L is the diameter of the glinting region, which we will assume is circular. For simplicity, we also assume that the two components are spatially distinct (i.e., the larger component is not a halo around the smaller one).

Vrba[4] measured a peak magnitude $m = 2^{\rm m}4$ on the night of 2 March 2009. The next night, the image saturated, and may have reached $m = 1^{\rm m}$. The two-parameter model described above fits both nights' interferometric data about equally well, with similar size scales and a similar division of flux between the two components, despite the difference in peak magnitude.

For the 2 March glint, we infer $A \sim 0.06$ and $\lesssim 0.004$ for the compact and extended components, respectively. If we assume that the peak brightness on 3 March was $1^{\rm m}5$, the corresponding albedo estimates are ~ 0.13 and $\lesssim 0.012$. For comparison, Vrba[4] estimated $A = 0.9$ in the 2 March data taken at the NOFS 1 m telescope and pointed out that for new solar panels, $A \approx 0.12$. It should be kept in mind that the albedos inferred from our interferometric data assume a circular geometry, but we have no information on the north-south extent of the glinting areas. If the "compact" component is extended north-south along the long dimension of the solar panels, the actual albedo is smaller than we estimate here. By contrast, the albedo of the extended component is quite small. We speculate that shiny multi-layer insulation, or MLI, covering the spacecraft bus and scattering sunlight in many directions, may be the cause of these low values.

5. NEXT STEPS

The results of these observations suggest several directions for further work. Perhaps the first is toward observing at lower spatial frequencies, since our results show that, at least during glints, the flux is mostly from extended structures. The NPOI is unlikely to commission short ($\lesssim 10$ m) baselines or an infrared detector in the near future, so using aperture masking techniques on 8 m class telescopes may be the most direct route to short-baseline observations. We are currently exploring this option.

Further steps include interferometric observations at infrared wavelengths with larger apertures, as well as increasing the number of apertures. In the infrared, albedos are higher, and the spatial frequency sampled by a given baseline is lower. Observing at these wavelengths with larger apertures could extend the observing season beyond the current glint season.

The greatest challenge will be acquiring data over a wide enough range of spatial frequencies to allow imaging of these complex objects. Detecting weak fringes at the higher spatial frequencies that characterize detailed structure will require multi-element interferometers with some means to phase the array, such as baseline bootstrapping.

Acknowledgments

REFERENCES

[1] Armstrong, J. T. et al., "The Navy Prototype Optical Interferometer," *Astrophys. J.* **496**, 550–571 (1998).

[2] Lambour, R., Bergemann, R., von Braun, C., and Gaposchkin, E. M., "Space-Based Visible Space Object Photometry: Initial Results," *J. Guidance, Control, and Dynamics* **23**(1), 159–164 (2000).

[3] Schaefer, B. E., Barber, M., Brooks, J. J., Deforrest, A., Maley, P. D., McLeod III, N. W., McNiel, R., Noymer, A. J., Presnell, A. K., Schwartz, R., and Whitney, S., "The Perseus Flasher and Satellite Glints," *Astrophys. J.* **320**, 398–404 (1987).

[4] Vrba, F. J., DiVittorio, M. E., Hindsley, R. B., Schmitt, H. R., Armstrong, J. T., Shankland, P. D., Hutter, D. J., and Benson, J. A., "A survey of geosynchronous satellite glints," in [*Proceedings of the Advanced Maui Optical and Space Surveillance Technologies Conference*], Ryan, S., ed., E28–E35 (2009). http://www.amostech.com/TechnicalPapers/2009.cfm.

[5] Armstrong, J. T., Hindsley, R. B., Restaino, S. R., Benson, J. A., Hutter, D. J., Vrba, F. J., Zavala, R. T., Gregory, S. A., and Schmitt, H. R., "Observations of a geosynchronous satellite with optical interferometry," in [*Adaptive Coded Aperture Imaging, Non-Imaging, and Unconventional Imaging Sensor Systems*], Rogers, S., Casasent, D. P., Dolne, J. J., Karr, T. J., and Gamiz, V. L., eds., *Proc. SPIE* **7468**, 74680K–74680K–9 (2009).